1 **Mutual effects of silver nanoparticles and antimony (III)/(V) co-exposed to**

2 **Glycine max (L.) Merr. in hydroponic system: uptake, translocation,**

3 **physiochemical responses and potential mechanisms**

4 Weicheng Cao[a,b], Jilai Gong[a,b,*], Guangming Zeng [a,b,*], Biao Song [a,b], Peng Zhang [a,b],

5 Juan Li [a,b], Siyuan Fang [a,b], Lei Qin [a,b], Jun Ye [c] and Zhe Cai [c]

6 *[a] College of Environmental Science and Engineering, Hunan University, Changsha*

7 *410082, P.R. China,*

8 *[b] Key Laboratory of Environmental Biology and Pollution Control, Hunan University,*

9 *Ministry of Education, Changsha 410082, P.R. China*

10 *[c] Hunan Qing Zhi Yuan Environmental Protection Technology Co., Ltd, Changsha*

11 *410082, P.R. China*

12

13 Pages: 29

14 Figures: 6

15 Tables: 2

16

17

18 * Corresponding author

19 E-mail address: jilaigong@gmail.com (J.L. Gong) and zgming@hnu.edu.cn (G. Zeng).

20

21 **Table S1.** Different exposure protocols of soybean to Ag NPs and Sb species in the
22 hydroponic system

Concentration (mg L^{-1})	Ag NPs 1	Ag NPs 2	Ag NPs 3	Ag NPs 4	Ag NPs 5
Sb (III) / Sb (V) 1	5+0.02(N 1)	5+0.10	5+0.20	5+0.65	5+1.0
Sb (III) / Sb (V) 2	10+0.02	10+0.10(N2)	10+0.20	10+0.65	10+1.0
Sb (III) / Sb (V) 3	25+0.02	25+0.10	25+0.20(N3)	25+0.65	25+1.0
Sb (III) / Sb (V) 4	50+0.02	50+0.10	50+0.20	50+0.65(N4)	50+1.0
Sb (III) / Sb (V) 5	100+0.02	100+0.10	100+0.20	100+0.65	100+1.0(N5)

23 * The concentration of Sb (III)/ Sb (V) ranged from 5–100 mg L^{-1} and the concentration of Ag NPs
24 ranged from 0.02–1 mg L^{-1}. The numbers after Ag NPs/Sb (1–5) present the concentration gradient.
25 The N1–N5 present the concentration gradients of combined exposure of Ag NPs with Sb (III)/Sb
26 (V).
27

28

29 **Table S2.** Abscission of leaves and cotyledons.

Treatments/ N5	AgNPs		AgNPs+Sb (III)		AgNPs+Sb (V)		Sb (III)		Sb (V)	
	Fall off	trait	Fall off	trait	Fall off	trait	Fall off	trait	Fall off	trait
Day 1	1 CL	NC	/	NC	1 leaf+1 CL	NC	/	NC	/	NC
Fresh weight (g)	0.0382		/		0.0657		/		/	
Day 2	/	NC	/	SY	3 cotyledons	SY	/	NC	/	NC
Fresh weight (g)	/		/		0.1085		/		/	
Day 3	/	NC	5 CLs	3 TSY	1 leaf+4 CLs	5 SLW	3 CL	7 SLW	/	3 SY
Fresh weight (g)	/		0.173		0.2436		0.2207		/	
Day 4	/	2 SLW	/	3 TSW	2 leaves+2 CL	1 TW+5 SLW	/	1 TW+2 SLW	/	3 SY+1 SLW
Fresh weight (g)	/		/		0.1951		/		/	
Day 5	1 CL	NC	3 CLs	1 TW+8 SLW	1 leaf	1 TW+6 LW	/	1 TW+2 LW+3 SLW	/	1 LW
Fresh weight (g)	0.0853		0.0664		0.0264		/		/	
Day 6	2 CL s	4 SLW	/	1 TW+8 DLW	/	1 TW+5 DLW	1 CL	1 TW+4 LW+4 SLW	1 leaf	1 LW+3 SLW
Fresh weight (g)	0.0419		/		/		0.023		0.0036	
Day 7	3 CL s	4 LW	7 CLs	3 TW	/	3 TW+6 DLW	3 CL s	1 TW+4 LW+4 SLW	/	4 LW
Fresh weight (g)	0.1169		0.3075		/		0.1379		/	
Total Fresh weight (g)	0.2823		0.5469		0.6393		0.3816		0.0036	

30 * CL presents the abbreviation for "cotyledon", NC is the abbreviation for "no obvious change", (T)SY is the

31 abbreviation for "(totally) slightly yellowing", T(S)W is the abbreviation for "total (slightly) withering of whole

32 plant" and (S/D) LW is the abbreviation for "(slightly/dramatically) leaf withering".

33
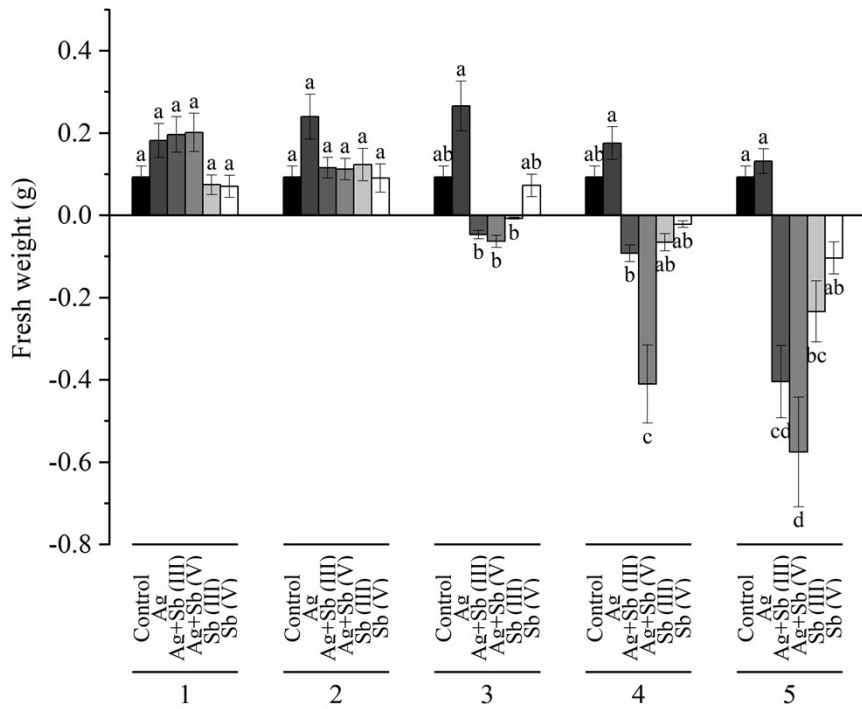
Figure S1. Effects of different treatments on fresh weight. The fresh weight of each treatment was significantly affected upon exposure to Ag NPs or/with Sb (III)/(V) with under different concentrations (see Table S1). Error bars indicate the mean standard deviation (n = 3) and different letters represent the significantly difference by *post hoc* Tukey's test multiple comparison ($p < 0.05$).
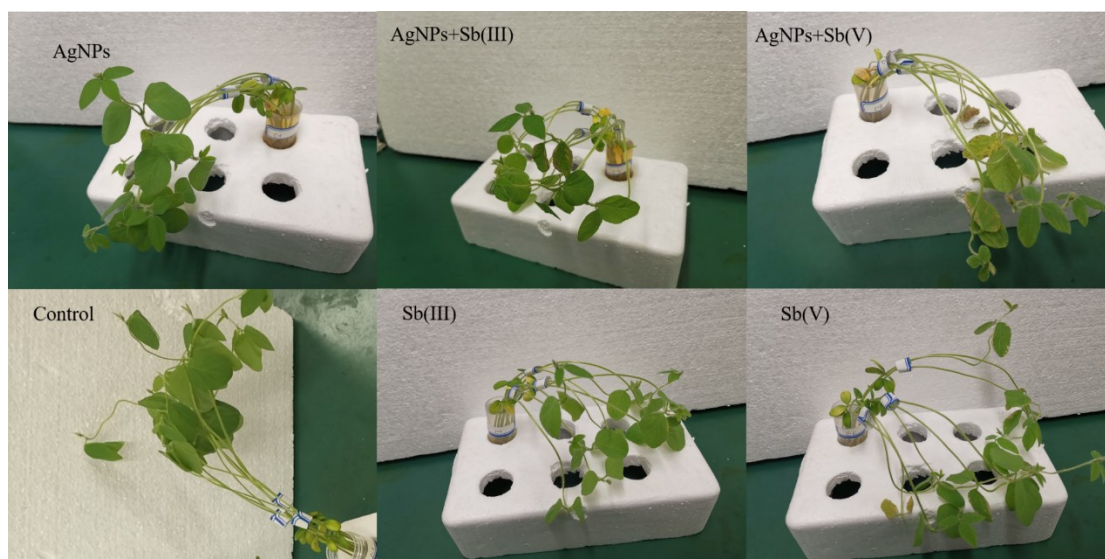
40

41 **Figure S2.** Photographs of soybean plantlets upon exposure to different treatments at

42 termination. Yellowing, brown spotting emerged on leaves and different luxuriant

43 degree of leaves could be observed.

44
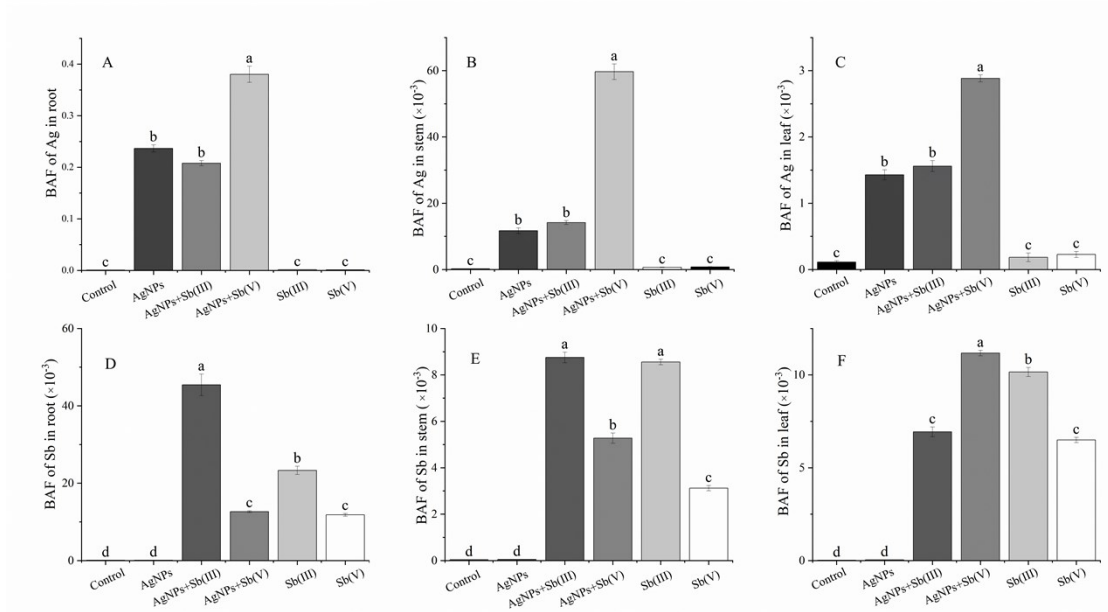
Figure S3. Bioaccumulation factors (BAF) of Ag (A, B, C) and Sb (D, E, F) in roots, stems and leave upon exposure to different treatments with Ag NPs or/with Sb (III) by N5 concentration. Error bars indicate the mean standard deviation (n = 3) and different letters represent the significantly difference by *post hoc* Tukey's test multiple comparison ($p < 0.05$).

52
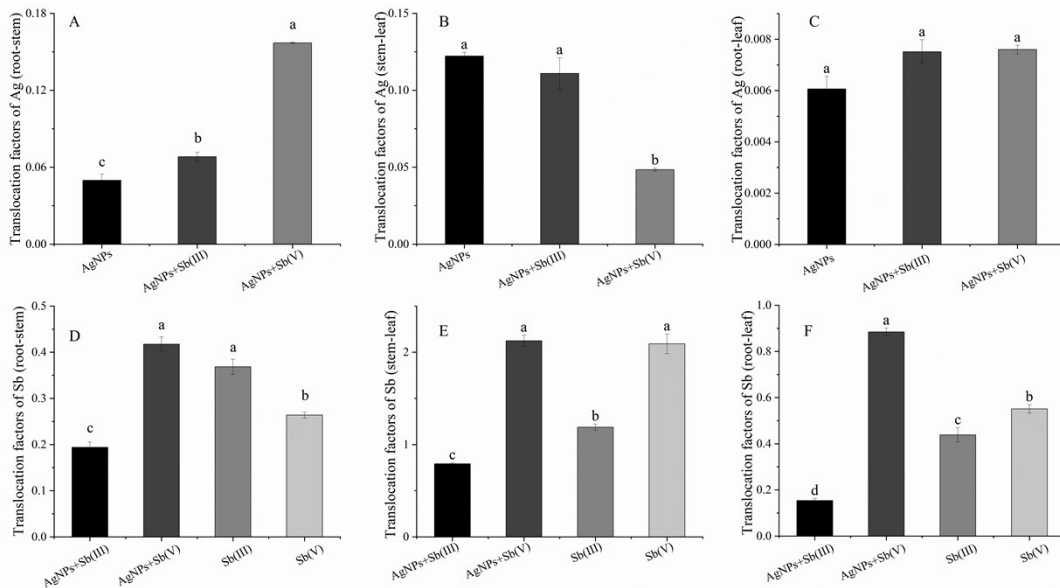
Figure S4. Translocation factors (TF) of Ag (A, B, C) and Sb (D, E, F) from roots to stems (TF_{r-s}), from stems to leaves (TF_{s-l}) and from roots to leaves (TF_{r-l}) upon exposure to different treatments with Ag NPs or/with Sb (III) by N5 concentration. Error bars indicate the mean standard deviation (n = 3) and different letters represent the significantly difference by *post hoc* Tukey's test multiple comparison ($p < 0.05$).
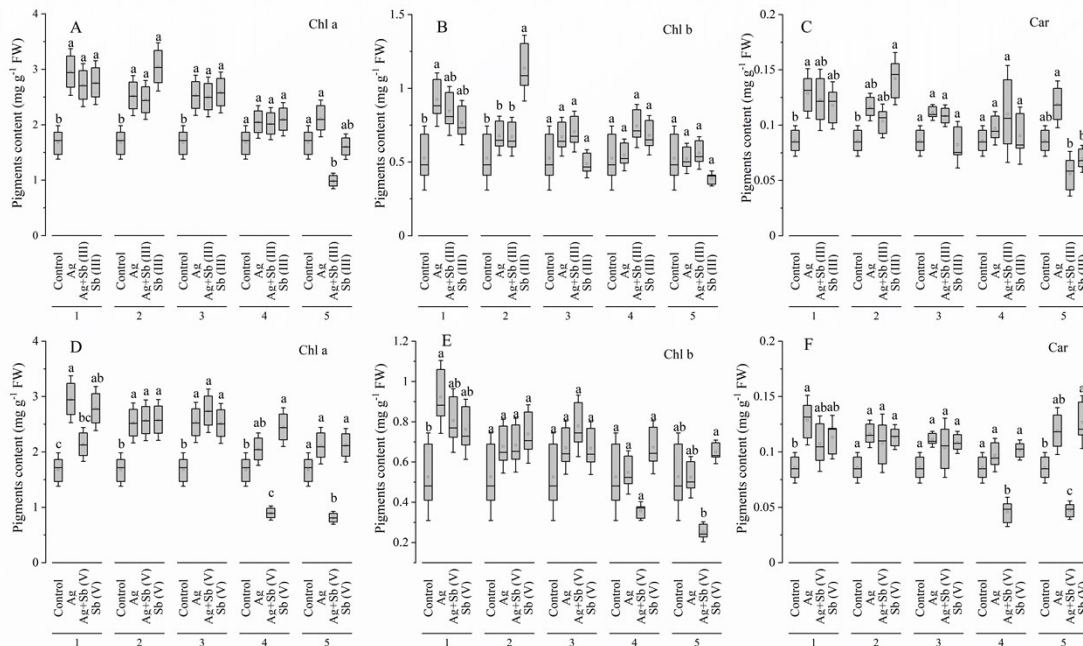
58
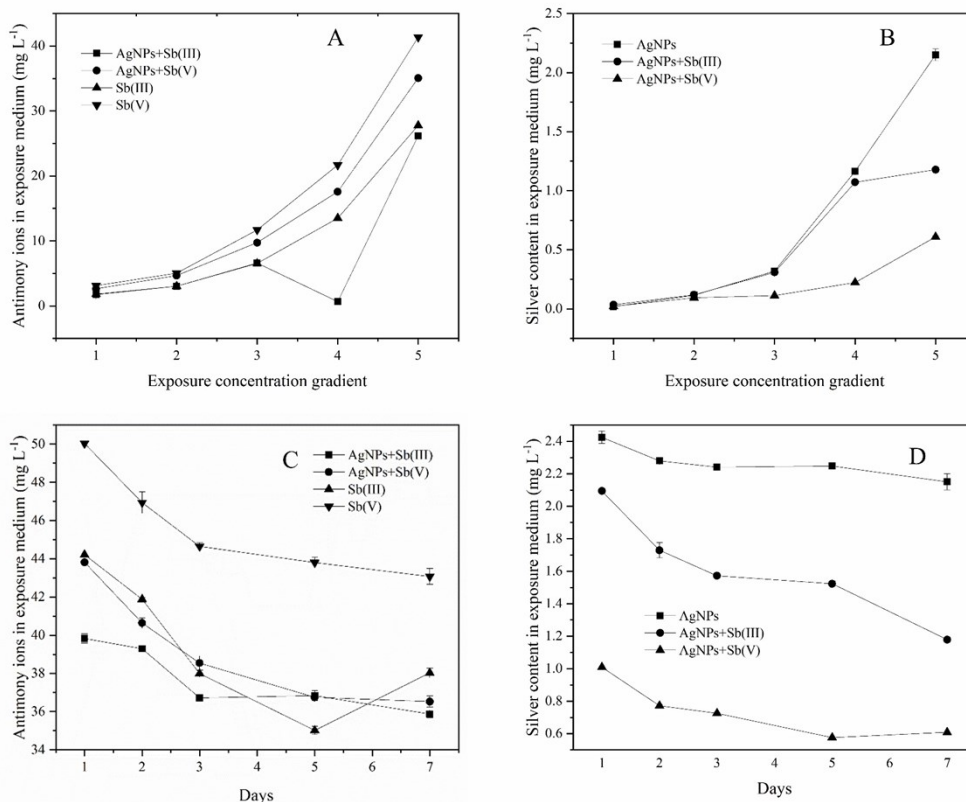
Figure S5. Residual Sb and Ag contents in culture medium when experiments terminated (A, B) and dynamic variation of Sb and Ag concentrations (see Table S1) in culture medium during the exposure period (C, D). All data were the means of three replicates (n = 3). Error bars indicate the mean standard deviation ($p < 0.05$).

Figure S6. Severely alteration of chlorophyll a, chlorophyll b, carotenoid contents exposed to different treatments with Ag NPs or/with Sb (III) by N1–N5 concentration (A, B, C), and Ag NPs or/with Sb (V) by N1–N5 concentrations (D, E, F). All the treatments displayed the significant promotion of pigment contents at low concentrations and gradually decreased with increasing concentration. Dots represent individual values, and boxplots display statistics (i.e., median, average, 25th and 75th percentile, and largest or smallest value extending from upper/lower quartile to 1.5-fold of the interquartile range). Error bars indicate the mean standard deviation (n = 3) and different letters represent the significantly difference by *post hoc* Tukey's test multiple comparison ($p < 0.05$).

77 **Supplemental experimental section**

78 Materials and methods

79 *Preparation of Ag NPs*

80   According to previous literature, PVP-coated Ag NPs were synthesized as

81 following.[1] Briefly, 15mL ethylene glycol (EG) containing 0.5g of PVP was heated up

82 to approximately 180 ℃ with vigorous stirring and kept for 30 min. Thereafter, when

83 the temperature was slowly adjusted to 120℃, 5 mL of EG containing 0.10 g $AgNO_3$

84 was dropwise added within 2 min and kept at 120℃ for another 3 min. The Ag NPs

85 were synthesized successfully with appearance of the brown colloidal dispersion

86 generation. Subsequently, the solution was cooled to ambient temperature and excess

87 acetone was added to generate a brown precipitate. In order to remove the free Ag ions,

88 the products were rinsed and centrifuged several times (20000rpm, 30min) for

89 purification. Finally, the as-synthesized nanoparticles were resuspended in deionized

90 water as stock solution. All suspensions were stored at 4 ℃ in dark. For measuring the

91 concentration of stock solution, one aliquot of the suspension was withdrawn and

92 diluted and measure the maximum absorbance value in the range $\lambda = 200–800$ nm. The

93 concentration of the stock solution was determined by Beer−Lambert's law.[2-4]

$$C = \frac{A}{\varepsilon L}$$

94   (1)

95 where C is the molar concentration of nanoparticle suspensions to be measured. A is

96 the absorbance of peak value of each measured sample. ε is the molar of silver

97 nanoparticle (cm^{-1} M^{-1}), which was determined according to previous literature. L is

98 the optical pathway length, which was counted as the length of the cuvette (1 cm) in

99   this study. Molar concentration of nanoparticles was converted from mM to mg L^{-1} for

100   the unification of units in this study.

101   Dynamic light scattering (DLS) for Z-average hydrodynamic diameter was

102   conducted by a Nano Zetasizer analyzer (Malvern Zetasizer Nano-ZS, Westborough,

103   MA). The absorbance of as-synthesized Ag NPs suspension was determined by surface

104   plasmon resonance spectra recorded over the range of 200–800 nm using ultraviolet-

105   visible spectrophotometer (UV-2550, Kyoto, Japan). As reported above[4], the

106   concentration of stock solution of Ag NPs was 30 mg L^{-1}.

107   *Plant Growth Conditions and Exposure Experiments*

108   *Glycine max* (Linn.) Merr. (soybean) seeds were obtained from commercial supplier.

109   The sterilized soybean seeds were firstly sowed in a seed tray which contained ultrapure

110   water underlying the grid layer and moist blotting paper overlaying seeds. For

111   germination, containers were transferred to a growth chamber (25-28 ℃) under

112   fluorescence intensity approximately 200 μmol m^{-2} s^{-1} photons flux, with a light/dark

113   cycle of 16 : 8 h for 3 days. After germination, the young seedlings were timely

114   transplanted into 50 mL centrifugal tubes and filled with 25% Hoagland nutrient

115   solution (pH 5.8). Then the containers were transferred into growth chamber with the

116   same culture conditions for another 2 weeks. During the growth of young seedlings, the

117   25% Hoagland nutrient solution decreased by the simultaneous effects of transpiration,

118   so the corresponding experimental nutrient solution should be compensated necessarily

119   to ensure the roots dipped in the hydroponics system. The daily transpiration rates were

120   observed and recorded in terms of the water loss in an photoperiod.[5]

121   After that, the plantlets were transferred from the tubes containing Hoagland solution

122 to the new tubes with ultrapure water for 2 days to remove the surface Hoagland

123 solution from root. Then the plantlets were amended with different treatments. In

124 details, the plants were exposed to different treatments containing various individual or

125 co-exposed conditions with corresponding concentration gradient except control

126 groups: (1) Ag NPs, (2) Ag NPs+Sb (III), (3) Ag NPs+Sb (V), (4) Sb (III) and (5) Sb

127 (V). The control and exposure treatments with respective combining forms were chosen

128 and noted as described in Table S1. The exposure concentrations of Ag ($\sim$ 0–1 mg L^{-1})

129 and Sb ($\sim$ 5–100 mg L^{-1}) were selected according to previous reports that could cause

130 slight toxicity alone to seedlings while enough to be detected in tissues.[6-8] These

131 protocols would be helpful to identify the independent and collaborative uptake and

132 accumulation of the two metal elements in plants, meanwhile the impacts of Sb

133 speciation on the dissolution of Ag NPs would be evaluated. Notably, the medium

134 solution was replaced by ultrapure water during the exposure period due to the potential

135 aggregation of Ag NPs induced by the high ionic strength of the Hoagland solution.[9]

136   The exposure treatments were sustained in the same cultivated condition for 7 days.

137 Fresh weight and transpiration loss were measured and recorded every photoperiod.

138 However, because of the individual specificity of each seeding, the transpiration loss of

139 each treatment was obviously different that the compensation using treatment solution

140 would lead to relatively greater deviation of cumulated exposure dosage.[5] Therefore,

141 the transpiration loss was replenished with ultrapure water instead of treatment

142 solutions and the dosage of water was determined according to the weight loss

143 monitored for each replicate over a 24 h interval. In the course of the exposures

144 performed, each treatment condition was triplicate prepared, and every replicate

145 contained at least six plantlets.

146 Determination of metal residue, uptake and distribution

147 The contents of Sb and Ag in medium

148   The total contents of different metallic element in solution and plant tissues were

149 determined by strong acid digestion, following Environmental Protection Agency

150 method no. 3050b (U.S) as previously reported.[10] The concentration of Ag^+ and Sb

151 dynamic variation in aqueous solution during exposure was measured by withdrawing

152 aliquots from each exposure medium at each photoperiod interval. Briefly, 0.1 mL-

153 aliquot of exposure medium of each treatment was withdrawn after every entire

154 photoperiod and collected in 10 mL centrifuge tubes. Then the subsamples were

155 digested with 1 mL of 70 % (v/v) HNO_3 at 90 °C for 2 hours and then diluted by 1%

156 nitric acid for quantification.

157 Sb and Ag contents in plant tissue

158   To evaluate the distribution of Ag and Sb in different plant tissues (including the

159 attached fraction on root surface), 50 mg (dry weight) of tissues were predigested with

160 2 mL of 70 % (v/v) nitric acid for overnight at room temperature. Then the blend was

161 further digested at 90 °C in a hot block for 4 h. After cooling to ambient temperature, 1

162 mL of 30 % hydrogen peroxide (H_2O_2) was added and incubated at 95 °C for another 2

163 h. Finally, the digestate was filtered using 0.22 μm sterile syringe filters (Millipore,

164 Billerica, MA, USA), then 0.5 mL of filtrate was withdrawn and diluted to 7 mL with

165　1 % (v/v) HNO$_3$. The total ion contents in different tissues were quantified by ICP-MS

166　spectrometry.

167　　Enzymatic digestion for extracting metal elements from roots was conducted on fresh

168　tissues to distinguish the dissolved and particulate fractions of Ag component following

169　the recently development protocol.[11-13] Freshly washed tissues of roots (0.2 g) were cut

170　into small pieces, and immersed into a centrifuge tube containing 3.6 mL of 20 Mm 2-

171　(N-morpholino) ethanesulfonic acid (MES) buffer (pH 5). A handheld homogenizer

172　was applied to homogenize the mixture thoroughly with subsequent addition of 0.4 mL

173　of 30 mg/mL Macerozyme R-10 enzyme (prepared in MES above). The mixture was

174　shaken in a vibrating incubator (New Brunswick Scientific, Edison, NJ) at 37℃ for 24

175　h.[5, 11] Afterwards, 2 mL aliquot of the digestate was centrifuged using the 10 kDa

176　centrifugal ultrafiltration (Amicon Ultra-4) at 4000 rpm for 10 min to separate the

177　dissolved contents from particulate fractions. The Ag ions in the filtrate was quantified

178　by ICP-MS and considered as the dissolved fractions of Ag in root tissues. While the

179　particulate fractions were calculated by the difference between total contents and ionic

180　contents of Ag.[14]

181　　Bioaccumulation factor (BAF), defined as the ratio of metal ion concentration in

182　plant tissues (root, stem, leaf) in response to the exposure concentration, was calculated

183　to compare and analyze the differences of Ag and Sb uptake in plants.[15] While the

184　translocation factor (TF) was calculated as the ratio of concentration of metal ions in

185　different plant tissues to assess the ions distribution and translocation in plants. The two

186　factors could be calculated by the equations as follows,[16, 17]

$$BAF = \frac{C_{root/stem/leaf}}{C_{ES}} \tag{2}$$

$$TF_{r-s} = \frac{C_{stem}}{C_{root}} \tag{3}$$

$$TF_{s-l} = \frac{C_{leaf}}{C_{stem}} \tag{4}$$

$$TF_{r-l} = \frac{C_{leaf}}{C_{root}} \tag{5}$$

where the $C_{root/stem/leaf}$ is the Ag or Sb ionic concentration in roots, stem and leaf respectively. C_{ES} represents the Ag or Sb ionic concentration in exposure system. TF_{r-s}, TF_{s-l}, and TF_{r-l} represents TF from roots to stems, from stems to leaves and from roots to leaves respectively.

Traits variation and Pigments analysis

The pigments contents (i.e., chlorophyll ($Chl\,a$, $Chl\,b$) and carotenoid (Car)), important indicators of photosynthesis efficiency and adverse physiological inhibition, were evaluated with slight modification according to previous protocol.[18, 19] In brief, fresh leaf tissue (50 mg) was divided into strips (ap. 0.2 cm $\times$ 1 cm) and added to centrifuge tubes containing 8 mL of 95 % ethanol/acetone (1:1, v/v) mixture solution. After incubated in dark for 8 h at room temperature, the absorbance (A) were measured by UV-vis spectrophotometer at the wavelengths of 470, 663 and 645 nm for calculating carotenoid and chlorophyll values. The calculation equations for chlorophyll and carotenoid were expressed as follows:[20-22]

$$Chlorophyll\ a\ (Chl\ a)\ (mg/g) = \frac{(12.21 \times A_{663} - 2.81 \times A_{646})V}{1000FW} \tag{6}$$

$$206 \qquad Chlorophyll\ b\ (Chl\ b)\ (mg/g) = \frac{(20.13 \times A_{646} - 5.03 \times A_{663})V}{1000FW} \qquad (7)$$

$$207 \qquad Total\ Chlorophyll\ (total\ Chl)\ (mg/g) = \frac{(7.18 \times A_{663} + 17.32 \times A_{646})V}{1000FW} \qquad (8)$$

$$208 \qquad Car(mg/g) = \frac{1000 \times A_{470} - 3.27 \times Chl\ a - 104 \times Chl\ b}{229 \times FW \times 1000} \qquad (9)$$

209 where A_{470}, A_{645} and A_{663} is the optical density at wavelength of 647, 663 and 645 nm

210 respectively; V is the volume of extracting solution (mL); FW is the fresh weight of

211 plant tissues (g).

212 Measurement of anthocyanin

213   Anthocyanin level in leaf was detected which was both related to the antioxidation

214 and light-relating process in plant.[23] In brief, 20 mg of fresh leaves were cut into pieces

215 (ap. 0.2 cm $\times$ 1 cm), and placed in 10 ml centrifuge tubes following amended with 1.2

216 ml of 2% HCl-MeOH solution. The tubes were sealed and incubated under

217 ultrasonication for 5 hours. After incubation, 0.8 ml of deionized water and 2 ml of

218 chloroform were added and fully mixed. Then the anthocyanin was separated from

219 chlorophylls by centrifuging at 16000 rpm for 5 min. The supernatant was collected

220 and the total anthocyanin contents were evaluated by the absorbance at 530 and 657

221 nm. The relative content of anthocyanin was calculated as the absorbance difference (

222 $A_{530} - A_{657}$) per gram fresh weight.[23, 24]

223 ROS accumulation in plant tissues

224   The production of ROS in plant tissues was determined by fluorescence staining

225 using an cell permeable indicator, 2',7'-dichlorodihydrofluorescein diacetate

226 (H$_2$DCFDA), as reported in previous literatures.[25, 26] Fresh tissues of different plant

227 parts from each treatment were weighted and washed three times with deionized water.

228 Then, the plant tissues were cut and transferred into 96 well-black plate containing 250

229 μL of 5 μM H₂DCFDA in deionized water for 30 min in the dark at 25 °C. The non-

230 fluorescent compound could be taken up by cells and hydrolyzed by cellular

231 endogenous esterases to the form of 2',7'-dichlorodihydrofluorescein (H₂DCF). The

232 reduced form of H₂DCF could be better trapped in cells and transformed into a highly

233 fluorescent probe, 2',7'-dichlorofluorescein (DCF), in the presence of ROS (especially

234 hydroperoxides).[26, 27] The accumulation of ROS in different plant tissues was measured

235 and recorded using a fluorescence microplate reader (Thermo Scientific Multiskan GO,

236 USA) at 530 nm fluorescence emission with the excitation wavelength of 485 nm.[18, 25]

237 The data of fluorescence intensity were normalized by fresh weight.

238 Lipid Peroxidation measurement

239 Lipid peroxidation usually occurred when plants was suffered from oxidative stress,

240 along with the production of malondialdehyde (MDA) which was considered as a direct

241 indicator of cellular damage and applied to evaluate the membrane integrity lever. The

242 method was slightly modified according to the protocol described by Devasagayam et.

243 al. (1987) and Jambunathan et. al. (2010).[28, 29] In details, plant tissues were weighted

244 (0.5 g) accurately and homogenized with 2 mL of 10 % (w/v) of tricholoroacetic acid

245 (TCA). Another 8 mL of TCA was added to make further homogenized. After

246 centrifuged at 4000 rpm for 15 min, the supernatant was collected and stored in 4℃.

247 Amout of 2 mL supernatant was placed in centrifuge tube and reacted with 2 mL of 0.6

248 % (w/v) of thiobarbituric acid (TBA) at 100 °C for 15 min. Then the reddish brown

249 solution was fast cooled down by ice-bath before measuring the absorbance at 450, 532,

250 and 600 nm. In addition, the reaction between MDA and TBA could be interfered by

251 soluble saccharides, therefore the MDA content was qualified by means of a

252 bicomponent analysis according to the Beer-Lambert's equation:

$$A_{450} = C_1 \times 85.4 \tag{10}$$

253

$$A_{532} - A_{600} = C_1 \times 7.4 + C_2 \times 155000 \tag{11}$$

254

255 The content of MDA was normalized with fresh weight:

$$C_1 (mol \, g^{-1}) = \frac{11.71 \times 10^{-3} \times A_{450}}{FW} \times V \tag{12}$$

256

$$C_2 (mol \, g^{-1}) = \frac{6.45 \times (A_{532} - A_{600}) - 0.56 \times A_{450}}{FW} \times 10^{-6} \times V \tag{13}$$

257

258 where A_{450}, A_{532}, A_{600} is the absorbance at 450, 532, and 600 nm respectively; V is

259 the volume of reaction solution (times by diluted ratio); C_1, C_2 is the content of

260 soluble saccharides and MDA ($mol \, g^{-1}$) reacting with TBA, respectively; FW

261 presents the fresh weight of plant tissues (g).

262 In addition, the soluble sugar content in exposure medium, which could be an

263 imprecise indicator of the damaged plasma-membrane permeability, was analyzed as

264 well for simply evaluating the toxic effects of different treatments. The soluble sugar

265 content was determined in terms of the anthracenone chromogenic reaction protocol.[30]

266 Briefly, 0.1 ml of exposure solution was withdrawn and diluted to 0.5 ml using

267 deionized water. The chromogenic reaction was performed by adding 2 mL of

268 anthracenone and boiling for 15 min. Then the absorbance was detected after cooling

269 to room temperature by a UV-vis spectrophotometer at the wavelengths of 620 nm.

270 Measurement of the activity of antioxidant enzymes

271 For observing the enzyme activities, roots, stems and leaves were separately

272 homogenized and centrifuged. The activity of superoxide dismutase (SOD) was

273 assayed following the protocol of SOD commercial kit (Nanjing Jiancheng, Nanjing,

274 China) by UV-Vis spectrophotometer[31]. One activity unit of SOD was expressed as the

275 50% reaction-inhibition of nitrobluetetrazolium (NBT) photoreduction in a 1 ml aliquot

276 of reaction solution according to the absorbance at 550 nm. The values were normalized

277 by fresh weight (FW) (U g^{-1} FW).

278 The peroxidase (POD) assay was performed according to the guaiacol oxidation

279 protocol under the presence of H_2O_2.[32] The absorbance of the oxidative product (4-o-

280 methoxyphenol) was measured at 470 nm to calculate the POD activity. In detail, 0.5 g

281 of plant tissues were accurately weighted and transferred into a mortar containing 0.2

282 g quartz sand and 0.5 ml PBS buffer solution. After sufficiently grinding, the

283 homogenate was transferred into a centrifuge tube. The mortar was rinsed with 5 mL

284 of deionized water and the rinse water was transfer into the same tube. After fixed to 8

285 mL, the tubes were centrifuged at 4℃ with 8000 rpm for 15 min. The supernatant was

286 stored at 4℃. Amount of 0.1 ml supernatant was mixed with 1 ml of guaiacol solution

287 (0.1%, v/v) and 1 ml of acetate buffer (pH = 5) in centrifuge tube containing 0.9 ml

288 deionized water. The mixture was fully homogenized and deposed in water-bath at 37℃

289 for 5 min following addition of 1 ml of H_2O_2 (0.08%, v/v). The absorbance was

290 measured at 470 nm 2 min later. The blank control for each sample was prepared as

291 described above while the H_2O_2 solution was replaced by deionized water. One unit of

292 POD activity was represented as the 0.01 units of absorbance change per minute per

293 milligram of fresh weight (U min^{-1} g^{-1} FW).

294   Owing to the ability of catalase (CAT) assay decomposing hydrogen peroxide

295 molecules into water and oxygen rapidly, the activity of CAT was defined as the 0.01

296 units of absorbance change of H_2O_2 per minute per milligram of fresh weight (U min^{-1}

297 g^{-1} FW) at 240 nm.[33] In details, 1 ml aliquot of phosphate buffer (pH = 7.8), 0.1 ml

298 aliquot of enzyme solution and 0.9 ml of deionized water were fully mixed in a 10 ml

299 centrifuge tube and treated in water-bath at 30℃ for 5 min. Thereafter, the absorbance

300 was immediately measured following addition of 1 ml aliquot of H_2O_2 solution (0.08%)

301 into the preheated tube at 240 nm. Blank control for each sample was prepared by

302 replacing the H_2O_2 solution with deionized water.

303 **Supplemental discussion**

304 *BAFs and TFs of Ag and Sb in plant tissues*

305   The BAF values presents the Ag or Sb bioaccumulation efficiency from exposure

306 solutions to plant tissues. Results indicated that, in indivial and combined exposure

307 systems, Ag and Sb were both primarily accumulated in roots (see Figure S3).

308 Additionally, the Ag accumulated in stems were higher than that in leaves, nevertheless,

309 the accumulations of Sb in stem and in leaves were in the same order of magnitude.

310   The translocation factors (TF$_{r-s}$, TF$_{s-l}$ and TF$_{r-l}$) were conducted to evaluate the transfer

311 ability of the elements in different tissue (Figure S4). On one hand, Sb (III) in individual

312 exposure system was more readily taken up and translocated from roots to stems. On

313 the other hand, Sb (V) in co-exposure system significantly promoted the translocation

314 of Ag from roots to stems while played significant inhibition of Ag from stems to

315 leaves. As comparison, Sb (III) in co-exposure system exhibited no obvious effects on

316 the translocation of Ag no matter from roots to stem or from stem to leaves. In addition,

317 both of Sb (III) or Sb (V) in co-exposure system led to no change of the translocation

318 of Ag from roots to leaves. According to the TFs of Sb, in individual exposure system,

319 Sb (V) resulted in higher efficiency translocation of Sb to leaves than Sb (III). The

320 results were in accordance with the reports by Zhou et al..[34] However, the translocation

321 factor values could be affected by different plant species, because different uptake

322 capacities and different dominate storage areas of Sb in different plants could lead to

323 the variety distribution of Sb in plants.[35, 36]

324   For co-exposure system, Ag NPs led to significant greater transfer of Sb from roots

325 to stems (by 58.1%) and then to leaves (by 60.7 %) when compared to that in individual

326 Sb (V) exposure system. Whereas, Ag NPs significantly restrained the Sb translocation

327 to stems and leaves by 47.3% and 65 % respectively. No obvious effects on the

328 translocation of Sb from stems to leaves were found in Ag NPs and Sb (V) co-exposure

329 system. Unexpected, the co-exposure of Ag NPs with Sb (III) significantly reduced the

330 translocation rate of Sb both from roots to stems and from stems to leaves (Figure S3

331 D~E). These results were identified as the effects of Ag NPs altering the Sb

332 bioavailability from hydroponic system to plants and both of Sb (V)/Sb (III) could

333 promote Ag transfer to plants though Sb (III) displayed very limited effects.

334 ***Sb and Ag concentrations in culture medium***

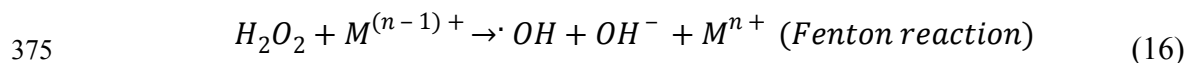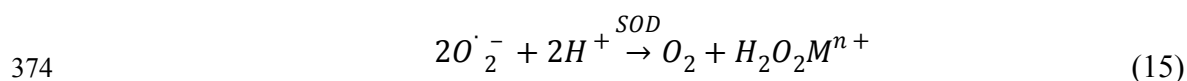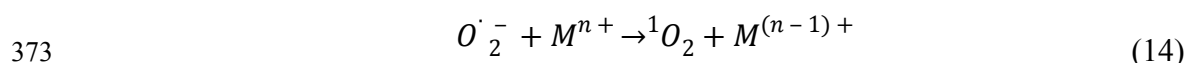335   Figure S4 (A and B) shows the Sb and Ag concentrations in medium after

336 experiments finished under the highest concentration exposure while the dynamic

337 changes of Sb and Ag concentrations during exposure period were displayed in Figure

338 S4 (C and D). Results showed that the concentrations of total Sb contents in different

339 treatment groups displayed an order, Sb (V) > Ag NPs+ Sb (V) > Sb (III) > Ag NPs+

340 Sb (III) after exposure (see Figure S5 A). Therefore, co-exposure Sb with Ag NPs could

341 be transferred into plant more efficiently than exposure to Sb individually. These results

342 were contributed to the effect of Ag NPs altering the Sb bioavailability and

343 accumulation from hydroponic system to plants under different treatments condition.

344 On the other hand, the presence of Sb under Ag NPs exposure also influenced the Ag

345 translocation to plant (Figure S5 C). Both Sb (V) and Sb (III) in co-exposure system

346 could promote the Ag contents transfer to plants when compared with that in Ag

347 individual exposure with concentration gradient increasing (shown in Figure S5 B).

348 Whereas, Sb (V) could result in significantly concentrations reduction of total Ag

349 residual up to -71.7 % (0.61mg L^{-1}) relative to the independent exposure of Ag NPs

350 (2.15 mg L^{-1}), while Sb (III) led to a relatively lower effect (-45.2 %, ap. 1.18mg L^{-1}).

351 As shown in Figure S5 (C and D), both the Sb and Ag contents in medium were

352 gradually decreased with the experiment time extending. The total Sb content variation

353 after experiments were reduced up to 56.9% for Sb (V) individual exposure, 61.9 % for

354 Sb (III) individual exposure, 63.5 % for Ag NPs and Sb (V) co-exposure, and 64.1 %

355 for Ag NPs and Sb (III) co-exposure respectively, indicating that Ag NPs could promote

356 the translocation of Sb species to plants, especially for Sb (V). Similar in Figure S5 D,

357 Ag contents exhibited a specific dynamic variation. In which, single Ag NPs treatment

358 resulted in about 42.7 % translocation at the end of experiments, as a contrast, Ag

359 contents in medium decreased about up to 83.8 % when treatment with Ag NPs with

360 Sb (V) co-exposure and up to 68.6 % translocation when treatment with Ag NPs with

361 Sb (III). These results were consistent with the conclusion in biomass increment

362 analysis, thus demonstrating the synergistic effects of Ag NPs and Sb leading to higher

363 accumulation both Ag and Sb contents in plants and greater negative biomass increment

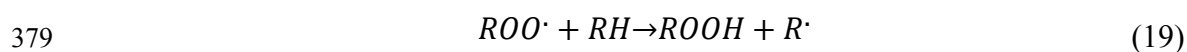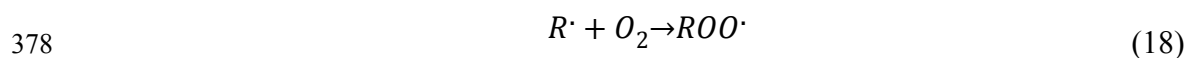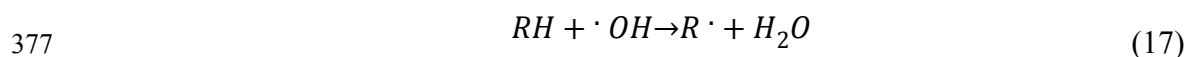364 relative to single treatments.

365 ***The potential generation for ROS***

366   In general, once excessive H_2O_2 are generated either from external abiotic stress or

367 alternatively from the defense process of SOD to superoxide anion radicals. Besides,

368 the ·OH very likely emerged during the detoxicating process of SOD to $O_2^{\cdot -}$ in which

369 ·OH could be generated by the Haber-Weiss reaction between $O_2^{\cdot -}$ and H_2O_2 or Fenton

370 reactions catalyzed by trace metal ions (Fe^{2+}, Cu^{2+} or Zn^{2+}),[15, 37, 38] leading to higher

371 MDA contents in plants and mediating serious peroxidation.[53, 101, 102]

372   Fenton-like Haber-Weiss reaction during SOD catalysis:[37-40]

$$O_2^{\cdot -} + M^{n+} \rightarrow {}^1O_2 + M^{(n-1)+} \tag{14}$$

$$2O_2^{\cdot -} + 2H^+ \xrightarrow{SOD} O_2 + H_2O_2 M^{n+} \tag{15}$$

$$H_2O_2 + M^{(n-1)+} \rightarrow {}^{\cdot}OH + OH^- + M^{n+} \ (Fenton\ reaction) \tag{16}$$

376   Initiation of lipid peroxidation,[41]

$$RH + {}^{\cdot}OH \rightarrow R^{\cdot} + H_2O \tag{17}$$

$$R^{\cdot} + O_2 \rightarrow ROO^{\cdot} \tag{18}$$

$$ROO^{\cdot} + RH \rightarrow ROOH + R^{\cdot} \tag{19}$$

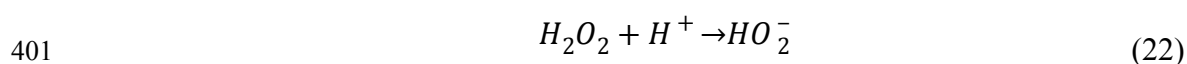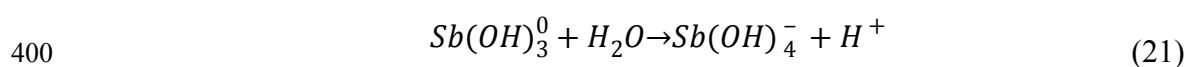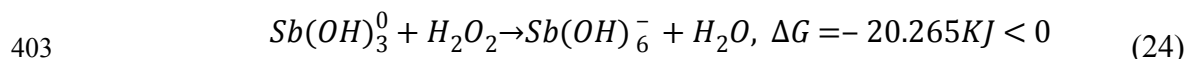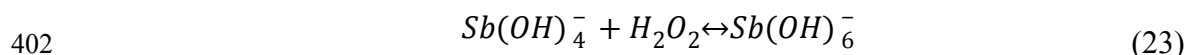$$ROO \cdot \rightarrow MDA + ethane \qquad (20)$$

380

381 where, M $^{n+}$ are the transition metals acting as electron acceptors such as Fe^{3+}/Sb^{5+}, RH

382 represents the unsaturated fatty acid while $R \cdot$ are the lipid free radicals.

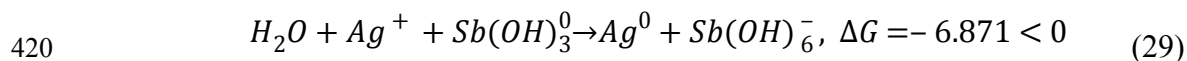383 ***Potential valence transformation of Ag NPs and Sb species***
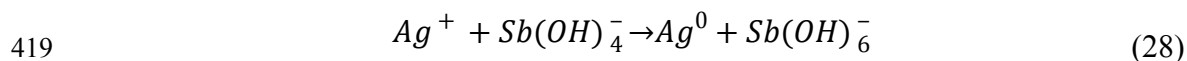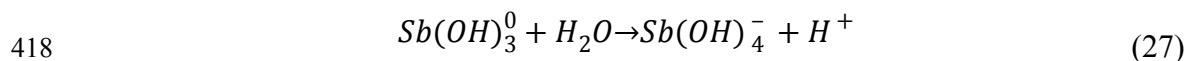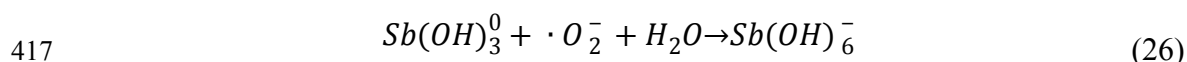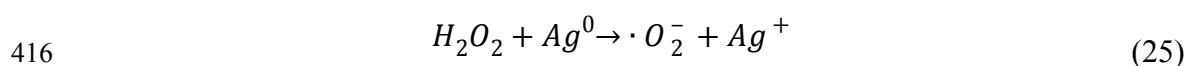
384   As described in this study, the phytotoxicity induced by single exposure of Ag NPs

385 and Sb (III)/(V) could be obviously enhanced by co-exposure of Ag NPs and Sb

386 (III)/(V). As reported, the phytotoxicity induced by Ag NPs were regarded as the

387 synergetic effects between Ag^+ and Ag NPs[42]. It was revealed that Ag^+ dissolved from

388 Ag NPs in environment occurred in cooperative oxidation involving protons and

389 dissolved oxygen according to the global reaction stoichiometry,[43] and the Ag^+ was

390 tightly correlated with bio-toxicity responses in organisms.[6, 44]

391   The bioavailability, uptake, and toxicity of Sb were quite determined by the oxidation

392 state and chemical speciation in aquatic systems.[45] Thus it was critical to understand

393 the speciation stability and transformation in exposure situations. Sb generally occurred

394 in two predominant oxidation states (i.e., Sb (III) and Sb (V)) , which was typical in

395 natural waters.[46, 47] As reported, Sb (III) was unstable which could be oxidized by O_2

396 or H_2O_2 upon exposure or even storage.[48] However, Sb oxidation kinetics had been

397 developed and validated that oxygen was not the driving force for Sb oxidation in

398 natural waters, but it was dependent on other oxidants (H_2O_2),[45, 48] which could be

399 described as follow equations.[2, 94]

400
$$Sb(OH)_3^0 + H_2O \rightarrow Sb(OH)_4^- + H^+ \qquad (21)$$

401
$$H_2O_2 + H^+ \rightarrow HO_2^- \qquad (22)$$

402
$$Sb(OH)_4^- + H_2O_2 \leftrightarrow Sb(OH)_6^-$$ (23)

403
$$Sb(OH)_3^0 + H_2O_2 \rightarrow Sb(OH)_6^- + H_2O, \ \Delta G = -20.265KJ < 0$$ (24)

404 However, when co-exposed with Sb (III), the reducibility of Ag NPs was deduced

405 for inhibition of the Sb oxidation process. According to the Standard Electrode

406 Potentials, the E^0 (Ag$^+$/Ag), E^0 (O$_2$/H$_2$O$_2$) and E^0 (Sb (OH)$_6^-$/Sb (OH)$_3^0$) were 0.7996,

407 0.659 and 0.764 V in circumneutral pH respectively, which exhibited the potential

408 redox interactions between Ag and Sb species though both of them were susceptible to

409 be oxidized by oxygen.[49, 50] Furthermore, the zero-valent Ag on the surface of Ag NPs

410 could promote the reduction of Sb (V) to Sb (III) and retard the oxidizing of Sb (III) to

411 Sb (V) by oxygen, which resulted in higher accumulation of Sb (III) in tissues and

412 greater damages in the co-exposure of Ag NPs with Sb (V) or Sb (III). In addition, the

413 interactions between Ag NPs and Sb species were deduced to modulate the dissolution

414 of Ag$^+$ from Ag NPs which correlated with Ag$^+$ accumulation in vivo and biochemical

415 responses. The interactions between Ag NPs and Sb could be expressed as follows:

416
$$H_2O_2 + Ag^0 \rightarrow \cdot O_2^- + Ag^+$$ (25)

417
$$Sb(OH)_3^0 + \cdot O_2^- + H_2O \rightarrow Sb(OH)_6^-$$ (26)

418
$$Sb(OH)_3^0 + H_2O \rightarrow Sb(OH)_4^- + H^+$$ (27)

419
$$Ag^+ + Sb(OH)_4^- \rightarrow Ag^0 + Sb(OH)_6^-$$ (28)

420
$$H_2O + Ag^+ + Sb(OH)_3^0 \rightarrow Ag^0 + Sb(OH)_6^-, \ \Delta G = -6.871 < 0$$ (29)

421 Accordingly, neither Sb (III) nor Sb (V) could promote the release of Ag ions. This

422 might be supported by the decreased ionic Ag contents in roots. The uptake of Sb had

423 been validated as a valence-dependent process and Sb predominately accumulated in

424 the roots of plants.[51] Ren et al. found that the concentrations of Sb (III) in exposure

425 medium and its accumulation in plant tissues in proportion to the total Sb were quite

426 higher than that exposed to Sb (V).[52] Whereas, the translocation efficiency of Sb (III)

427 were lower than that of Sb (V) though it might be dependent on the species of plant.[53]

428 Additionally, the phytotoxicity and selective uptake had also been reported to be

429 dependent on plant species in which Sb (V) could exhibited higher toxicity than Sb (III)

430 treatments.[54]

Reference

432 1.   Li, L.; Sun, J.; Li, X.; Zhang, Y.; Wang, Z.; Wang, C.; Dai, J.; Wang, Q.,
433 Controllable synthesis of monodispersed silver nanoparticles as standards for
434 quantitative assessment of their cytotoxicity. *Biomaterials* **2012,** *33* (6), 1714-21.
435 2.   Shang, J.; Gao, X., Nanoparticle counting: towards accurate determination of the
436 molar concentration. *Chemical Society reviews* **2014,** *43* (21), 7267-7278.
437 3.   Navarro, J. R.; Werts, M. H., Resonant light scattering spectroscopy of gold, silver
438 and gold-silver alloy nanoparticles and optical detection in microfluidic channels.
439 *Analyst* **2013,** *138* (2), 583-592.
440 4.   Paramelle, D.; Sadovoy, A.; Gorelik, S.; Free, P.; Hobley, J.; Fernig, D. G., A rapid
441 method to estimate the concentration of citrate capped silver nanoparticles from UV-
442 visible light spectra. *Analyst* **2014,** *139* (19), 4855-4861.
443 5.   Rossi, L.; Sharifan, H.; Zhang, W.; Schwab, A. P.; Ma, X., Mutual effects and in
444 planta accumulation of co-existing cerium oxide nanoparticles and cadmium in
445 hydroponically grown soybean (Glycine max (L.) Merr.). *Environmental Science:*
446 *Nano* **2018,** *5* (1), 150-157.
447 6.   Wang, J.; Koo, Y.; Alexander, A.; Yang, Y.; Westerhof, S.; Zhang, Q.; Schnoor,
448 J. L.; Colvin, V. L.; Braam, J.; Alvarez, P. J., Phytostimulation of poplars and
449 Arabidopsis exposed to silver nanoparticles and Ag$^+$ at sublethal concentrations.
450 *Environmental science & technology* **2013,** *47* (10), 5442-5449.
451 7.   WHO, Antimony in Drinking Water. Background Document for Development of
452 WHO Guidelines for Drinking Water Quality. WHO/SDE/WSH/03, 04/74. World
453 Health Organization, Geneva. **2003**.
454 8.   Müller, K.; Daus, B.; Mattusch, J.; Vetterlein, D.; Merbach, I.; Wennrich, R.,
455 Impact of arsenic on uptake and bio-accumulation of antimony by arsenic
456 hyperaccumulator Pteris vittata. *Environmental pollution* **2013,** *174*, 128-133.
457 9.   Li, X.;   Lenhart, J. J.; Walker, H. W., Aggregation kinetics and dissolution of
458 coated silver nanoparticles. *Langmuir* **2012,** *28* (2), 1095-1104.
459 10. USEPA, Acid Digestion of Sediments, Sludges, and Soils, in Test Methods for

460 Evaluating Solid Waste Physical. *SW-846, Environmental Protection Agency, Office of*
461 *Solid Waste,* **1996**, p. 12.

462 11. Stowers, C.; King, M.; Rossi, L.; Zhang, W.; Arya, A.; Ma, X., Initial Sterilization
463 of Soil Affected Interactions of Cerium Oxide Nanoparticles and Soybean Seedlings
464 (Glycine max (L.) Merr.) in a Greenhouse Study. *ACS Sustainable Chemistry &*
465 *Engineering* **2018,** *6* (8), 10307-10314.

466 12. Zhang, W.; Dan, Y.; Shi, H.; Ma, X., Elucidating the mechanisms for plant uptake
467 and in-planta speciation of cerium in radish (Raphanus sativus L.) treated with cerium
468 oxide nanoparticles. *Journal of Environmental Chemical Engineering* **2017,** *5* (1), 572-
469 577.

470 13. Dan, Y.; Zhang, W.; Xue, R.; Ma, X.; Stephan, C.; Shi, H., Characterization of
471 gold nanoparticle uptake by tomato plants using enzymatic extraction followed by
472 single-particle inductively coupled plasma-mass spectrometry analysis. *Environmental*
473 *science & technology* **2015,** *49* (5), 3007-3014.

474 14. Li, C. C.; Dang, F.; Li, M.; Zhu, M.; Zhong, H.; Hintelmann, H.; Zhou, D. M.,
475 Effects of exposure pathways on the accumulation and phytotoxicity of silver
476 nanoparticles in soybean and rice. *Nanotoxicology* **2017,** *11* (5), 699-709.

477 15. Ma, C.; White, J. C.; Dhankher, O. P.; Xing, B., Metal-based nanotoxicity and
478 detoxification pathways in higher plants. *Environmental science & technology* **2015,**
479 *49* (12), 7109-7122.

480 16. Wang, X.; Li, F.; Yuan, C.; Li, B.; Liu, T.; Liu, C.; Du, Y.; Liu, C., The
481 translocation of antimony in soil-rice system with comparisons to arsenic: Alleviation
482 of their accumulation in rice by simultaneous use of Fe(II) and NO3-. *The Science of*
483 *the total environment* **2019,** *650* (Pt 1), 633-641.

484 17. Wan, X.; Yang, J.; Lei, M., Speciation and uptake of antimony and arsenic by
485 two populations of Pteris vittata L. and Holcus lanatus L. from co-contaminated soil.
486 *Environmental science and pollution research international* **2018,** *25* (32), 32447-
487 32457.

488 18. Jiang, H. S.; Yin, L. Y.; Ren, N. N.; Zhao, S. T.; Li, Z.; Zhi, Y.; Shao, H.; Li, W.;
489 Gontero, B., Silver nanoparticles induced reactive oxygen species via photosynthetic
490 energy transport imbalance in an aquatic plant. *Nanotoxicology* **2017,** *11* (2), 157-167.

491 19. Moran, R., Formulae for determination of chlorophyllous pigments extracted with
492 n,n-dimethylformamide. *Plant physiology* **1982,** *69* (6), 1376-1381.

493 20. Ma, C.; Chhikara, S.; Minocha, R.; Long, S.; Musante, C.; White, J. C.; Xing,
494 B.; Dhankher, O. P., Reduced Silver Nanoparticle Phytotoxicity in Crambe abyssinica
495 with Enhanced Glutathione Production by Overexpressing Bacterial gamma-
496 Glutamylcysteine Synthase. *Environmental science & technology* **2015,** *49* (16),
497 10117-10126.

498 21. Wellburn, A. R.; Lichtenthaler, H., Formulae and Program to Determine Total
499 Carotenoids and Chlorophylls A and B of Leaf Extracts in Different Solvents. In
500 *Advances in Photosynthesis Research: Proceedings of the VIth International Congress*
501 *on Photosynthesis, Brussels, Belgium, August 1–6, 1983 Volume 2*, Sybesma, C., Ed.
502 Springer Netherlands: Dordrecht, 1984; pp 9-12.

503 22. Rossi, L.; Zhang, W.; Schwab, A. P.; Ma, X., Uptake, Accumulation, and in

Planta Distribution of Coexisting Cerium Oxide Nanoparticles and Cadmium in Glycine max (L.) Merr. *Environmental science & technology* **2017,** *51* (21), 12815-12824.

23. Yoo, J.; Shin, D. H.; Cho, M.-H.; Kim, T.-L.; Bhoo, S. H.; Hahn, T.-R., An ankyrin repeat protein is involved in anthocyanin biosynthesis in Arabidopsis. *Physiol Plant* **2011,** *142* (4), 314-325.

24. Fankhauser, C.; Casal, J. J., Phenotypic characterization of a photomorphogenic mutant. *The Plant journal : for cell and molecular biology* **2004,** *39* (5), 747-760.

25. Oukarroum, A.; Barhoumi, L.; Pirastru, L.; Dewez, D., Silver nanoparticle toxicity effect on growth and cellular viability of the aquatic plant Lemna gibba. *Environ Toxicol Chem* **2013,** *32* (4), 902-907.

26. Greenberg, B. M.; Dixon, D. G.; Lampi, M. A.; Tripuranthakam, S.; Babu, T. S.; Akhtar, T. A., Similar Stress Responses are Elicited by Copper and Ultraviolet Radiation in the Aquatic Plant Lemna gibba: Implication of Reactive Oxygen Species as Common Signals. *Plant and Cell Physiology* **2003,** *44* (12), 1320-1329.

27. Wiederschain, G. Y., The Molecular Probes handbook. A guide to fluorescent probes and labeling technologies. *Biochemistry (Moscow)* **2011,** *76* (11), 1276-1276.

28. Devasagayam, T. P. A.; Tarachand, U., Decreased lipid peroxidation in the rat kidney during gestation. *Biochemical and biophysical research communications* **1987,** *145* (1), 134-138.

29. Jambunathan, N., Determination and Detection of Reactive Oxygen Species (ROS), Lipid Peroxidation, and Electrolyte Leakage in Plants. In *Plant Stress Tolerance: Methods and Protocols*, Sunkar, R., Ed. Humana Press: Totowa, NJ, 2010; pp 291-297.

30. Yemm, E. W.; Willis, A. J., The estimation of carbohydrates in plant extracts by anthrone. *The Biochemical journal* **1954,** *57* (3), 508-514.

31. Rico, C. M.; Hong, J.; Morales, M. I.; Zhao, L.; Barrios, A. C.; Zhang, J.-Y.; Peralta-Videa, J. R.; Gardea-Torresdey, J. L., Effect of Cerium Oxide Nanoparticles on Rice: A Study Involving the Antioxidant Defense System and In Vivo Fluorescence Imaging. *Environmental science & technology* **2013,** *47* (11), 5635-5642.

32. Maehly, A. C., *Plant Peroxidases: Methods in Enzymology.* Methods in Enzymology: 2019.

33. Li, X.; Ke, M.; Zhang, M.; Peijnenburg, W.; Fan, X.; Xu, J.; Zhang, Z.; Lu, T.; Fu, Z.; Qian, H., The interactive effects of diclofop-methyl and silver nanoparticles on Arabidopsis thaliana: Growth, photosynthesis and antioxidant system. *Environmental pollution* **2018,** *232*, 212-219.

34. Zhou, X. J.; Sun, C. Y.; Zhu, P. F.; Liu, F., Effects of Antimony Stress on Photosynthesis and Growth of Acorus calamus. *Frontiers in Plant Science* **2018,** *9*, 579.

35. Feng, R.; Wei, C.; Tu, S.; Wu, F.; Yang, L., Antimony accumulation and antioxidative responses in four fern plants. *Plant and Soil* **2008,** *317* (1-2), 93-101.

36. Tisarum, R.; Lessl, J. T.; Dong, X.; de Oliveira, L. M.; Rathinasabapathi, B.; Ma, L. Q., Antimony uptake, efflux and speciation in arsenic hyperaccumulator Pteris vittata. *Environmental pollution* **2014,** *186*, 110-114.

37. Freinbichler, W.; Colivicchi, M. A.; Stefanini, C.; Bianchi, L.; Ballini, C.;

548 Misini, B.; Weinberger, P.; Linert, W.; Varešlija, D.; Tipton, K. F.; Della Corte,
549 L., Highly reactive oxygen species: detection, formation, and possible functions.
550 *Cellular Molecular Life Sciences* **2011,** *68* (12), 2067-2079.
551 38. Yim, M. B.; Boon Chock, P.; Stadtman, E. R., Cu,Zn superoxide dismutase
552 catalyzes hydroxyl radical production from hydrogen peroxide. *Free Radical Biology*
553 *and Medicine* **1990,** *9*, 43.
554 39. Upham, B. L.; Jahnke, L. S., Photooxidative reactions in chloroplast thylakoids.
555 Evidence for a Fenton-type reaction promoted by superoxide or ascorbate.
556 *Photosynthesis Research* **1986,** *8* (3), 235-247.
557 40. Gill, S. S.; Tuteja, N., Reactive oxygen species and antioxidant machinery in
558 abiotic stress tolerance in crop plants. *Plant physiology and biochemistry : PPB* **2010,**
559 *48* (12), 909-930.
560 41. SHIMOMURA; Osamu, Y., Superoxlde-triggered Chemiluminescence of the
561 Extract of Luminous Mushroom (Panellus stipticus) after Treatment with Methylamine.
562 *Journal of Experimental Botany* **1991,** *42* (237), 555-560.
563 42. Miao, A. J.; Luo, Z.; Chen, C. S.; Chin, W. C.; Santschi, P. H.; Quigg, A.,
564 Intracellular uptake: a possible mechanism for silver engineered nanoparticle toxicity
565 to a freshwater alga Ochromonas danica. *PloS one* **2010,** *5* (12), e15196.
566 43. Liu, J.; Hurt, R. H., Ion release kinetics and particle persistence in aqueous nano-
567 silver colloids. *Environmental science & technology* **2010,** *44* (6), 2169-2175.
568 44. Yin, L.; Cheng, Y.; Espinasse, B.; Colman, B. P.; Auffan, M.; Wiesner,
569 M.; Rose, J.; Liu, J.; Bernhardt, E. S., More than the ions: the effects of silver
570 nanoparticles on Lolium multiflorum. *Environmental science & technology* **2011,** *45*
571 (6), 2360-2367.
572 45. Obiakor, M. O.; Tighe, M.; Pereg, L.; Wilson, S. C., Bioaccumulation,
573 trophodynamics and ecotoxicity of antimony in environmental freshwater food webs.
574 *Critical Reviews in Environmental Science and Technology* **2018,** *47* (22), 2208-2258.
575 46. Filella, M.; Belzile, N.; Chen, Y.-W., Antimony in the environment: a review
576 focused on natural waters: I. Occurrence. *Earth-Science Reviews* **2002,** *57* (1), 125-176.
577 47. Pierart, A.; Shahid, M.; Séjalon-Delmas, N.; Dumat, C., Antimony
578 bioavailability: Knowledge and research perspectives for sustainable agricultures.
579 *Journal of Hazardous Materials* **2015,** *289*, 219-234.
580 48. Herath, I.; Vithanage, M.; Bundschuh, J., Antimony as a global dilemma:
581 Geochemistry, mobility, fate and transport. *Environmental pollution* **2017,** *223*, 545-
582 559.
583 49. Filella, M.; May, P. M., Computer simulation of the low-molecular-weight
584 inorganic species distribution of antimony(III) and antimony(V) in natural waters.
585 *Geochimica et Cosmochimica Acta* **2003,** *67* (21), 4013-4031.
586 50. Kulp, T. R.; Miller, L. G.; Braiotta, F.; Webb, S. M.; Kocar, B. D.; Blum,
587 J. S.; Oremland, R. S., Microbiological reduction of Sb(V) in anoxic freshwater
588 sediments. *Environmental science & technology* **2014,** *48* (1), 218-226.
589 51. Vaculik, M.; Mrazova, A.; Lux, A., Antimony (SbIII) reduces growth, declines
590 photosynthesis, and modifies leaf tissue anatomy in sunflower (Helianthus annuus L.).
591 *Environmental science and pollution research international* **2015,** *22* (23), 18699-706.

592 52. Ren, J. H.; Ma, L. Q.; Sun, H. J.; Cai, F.; Luo, J., Antimony uptake, translocation
593 and speciation in rice plants exposed to antimonite and antimonate. *The Science of the*
594 *total environment* **2014,** *475*, 83-89.
595 53. Tisarum, R.; Lessl, J. T.; Dong, X.; de Oliveira, L. M.; Rathinasabapathi, B.; Ma,
596 L. Q., Antimony uptake, efflux and speciation in arsenic hyperaccumulator Pteris
597 vittata. *Environmental pollution* **2014,** *186*, 110-114.
598 54. Shtangeeva, I.; Steinnes, E.; Lierhagen, S., Uptake of different forms of antimony
599 by wheat and rye seedlings. *Environmental Science Pollution Research* **2012,** *19* (2),
600 502-509.
601